THE JOURNAL OF PHYSICAL CHEMISTRY B

Article

pubs.acs.org/JPCB

Spectroscopic Study of the Light-Harvesting CP29 Antenna Complex of Photosystem II—Part I

Ximao Feng,[†] Xiaowei Pan,[‡] Mei Li,[‡] Jörg Pieper,[§] Wenrui Chang,[‡] and Ryszard Jankowiak*[,†,∥,⊥]

[†]Department of Chemistry, Kansas State University, Manhattan, Kansas 66506, United States

[‡]National Laboratory of Biomacromolecules, Institute of Biophysics, Chinese Academy of Sciences, Beijing, China

[§]Institute of Physics, University of Tartu, Tartu, Estonia

[∥]Faculty of Applied Physics and Mathematics, Gdańsk University of Technology, Gdańsk, Poland

ABSTRACT: Recent structural data revealed that the CP29 protein of higher plant photosystem II (PSII) contains 13 chlorophylls (Chl's) per complex (Pan et al. *Nat. Struct. Mol. Biol.* **2011**, *18*, 309), i.e., five Chl's more than in the predicted CP29 homology-based structure model (Bassi et al. *Proc. Natl. Acad. Sci. U.S.A.* **1999**, *96*, 10056). This lack of consensus presents a constraint on the interpretation of CP29 optical spectra and their underlying electronic structure. To address this problem, we present new low-temperature (5 K) absorption, fluorescence, and hole-burned (HB) spectra for CP29 proteins from spinach, which are compared with the previously reported data. We focus on excitation energy transfer (EET) and the nature of the lowest-energy state(s). We argue that CP29 proteins previously studied by HB spectroscopy lacked at least one Chl *a* molecule (i.e., *a*615 or *a*611), which along with Chl *a*612 contribute to the lowest energy state in more intact CP29, and one Chl *b* (most likely *b*607). This is why the low-energy state and fluorescence maxima reported by Pieper et al. (*Photochem. Photobiol.* **2000**, *71*, 574) were blue-shifted by ~1 nm, the low-energy state appeared to be highly localized on a single Chl *a* molecule, and the position of the low-energy state was independent of burning fluence. In contrast, the position of the nonresonant HB spectrum shifts blue with increasing fluence in intact CP29, as this state is strongly contributed to by several pigments (i.e., *a*611, *a*612, *a*615, and *a*610). Zero-phonon hole widths obtained for the Chl *b* band at 638.5 nm (5 K) revealed two independent Chl *b* → Chl *a* EET times, i.e., 4 ± 0.5 and 0.4 ± 0.1 ps. The latter value is a factor of 2 faster than previously observed by HB spectroscopy and very similar to the one observed by Gradinaru et al. (*J. Phys. Chem. B* **2000**, *104*, 9330) in pump−probe experiments. EET time from 650 nm Chl *b* → Chl *a* and downward EET from Chl(s) *a* state(s) at 665 nm occurs in 4.9 ± 0.7 ps. These findings provide important constraints for excitonic calculations that are discussed in the accompanying paper (part II, DOI 10.1021/jp4004278).

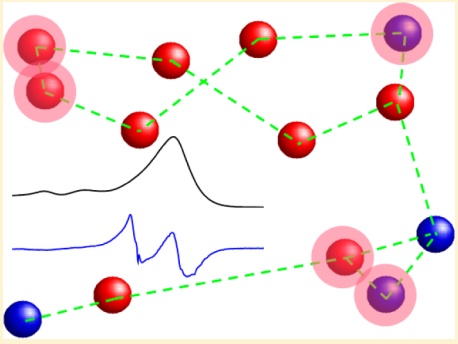

1. INTRODUCTION

Photosynthesis in higher plants and green algae is initiated by light-harvesting of the antenna systems in photosystem II (PSII). The light-harvesting pigment−protein complexes in PSII fall into two categories: core antenna and peripheral antenna.[1−5] CP47 and CP43 are called core antenna because they are located just outside of the reaction center (RC) complex of PSII, and they, together with the RC, form the so-called PSII core complex.[6,7] These two core complexes are responsible for light-harvesting and funneling the excitation energy from the peripheral antennas to the RC. The peripheral antennas, situated outside of the core antenna, include LHCII (Lhcb1−3),[8] CP29 (Lhcb4),[9,10] CP26 (Lhcb5), and CP24 (Lhcb6)[11] complexes. While the major complex LHCII exists in trimeric form in Nature, the three minor antenna complexes are usually monomeric. Until recently,[12] the consensus was that the CP29 complex contains only eight pigments; the latter was based on studies of extracted and purified CP29 assuming two carotenoid molecules per complex,[13−15] which was subsequently compared with the reconstituted complex.[16]

Recent X-ray structural studies of the CP29 complex from spinach[12] demonstrated that each CP29 monomer has 13 chlorophylls (Chl's), i.e., eight Chl *a*, four Chl *b*, and likely one mixed Chl *a*/Chl *b* site. It appears the 13 Chl molecules form four major domains: domain 1: *a*602, *a*603, *a*608, *b*609, *a*610, *a*611, *a*612, and *a*615 Chl's; domains 2 and 2′: each with one Chl, i.e., *a*613 and *b*614, respectively; and domain 3: *a*604, *b*606 and *b*607.[12] The couplings between pigments in two different domains and between the cofactors on the stromal and luminal sides are small, less than 10 cm^{-1} (see Table A1 in the Appendix). Domains 2, 2′, and 3 are located on the luminal side, with the remaining pigments on the stromal side (domain 1). As shown in Figure 1A, the four Chl *b* molecules are located at three different domains, with three of them on the luminal side. Mixed-pigment composition ensures absorption of light energy in a broad spectral range. Note that Chl's *b*607 and *b*608 as well as *a*604, *a*611, and *a*615 (indicated by a black

Received: January 14, 2013
Revised: April 3, 2013

   dx.doi.org/10.1021/jp4004328 | *J. Phys. Chem. B* XXXX, XXX, XXX−XXX

Table 1. Comparison of Pigment Composition in the CP29 Complex Based on refs 12 and 13[a]

LHCII[17]	CP29[12]	CP29[13]
*b*601		
*a*602	*a*602	A4 (*a*)
*a*603	*a*603	A5 (*a*)
*a*604	*a*604	
*b*605		
*b*606	*b*606	B6 (*a*/*b*)
*b*607	*b*607	
*b*608	*b*608	
*b*609	*a*609	B5 (*a*/*b*)
*a*610	*a*/*b*610	A1 (*a*)
*a*611	*a*611	
*a*612	*a*612	A2 (*a*)
*a*613	*a*613	A3 (*a*/*b*)
*a*614	*b*614	B3 (*a*/*b*)
	*a*615	

[a]Pigment composition in the LHCII antenna complex (left column) is shown for comparison.[17] Note that *a* and *b* in the left two columns refer to Chl *a* and Chl *b*, respectively. In the third column, A and B are used to show the binding sites, while their Chl identities are given in the following brackets.[13]

rectangle) were absent in the predicted CP29 model based on site directed mutagenesis studies.[13] These newly identified Chl's use either water molecules or glycerol-3-phosphate as their central ligands and might be lost in the reconstituted sample.

Within domains 1 and 3 of the CP29 complex, the inter-pigment electronic couplings (V_{nm}) are usually strong. In the *a*612−*a*611−*a*615 trimer of domain 1, Chl *a*611 has very strong coupling with both *a*612 and *a*615 pigments (>85 cm^{-1}), while the strongest coupling is between Chl's *a*611 and *a*615 (96 cm^{-1}). In the second trimer of domain 1, i.e., Chl's *a*603−*a*609−*b*608, the strongest coupling is between Chl *a*603 and *a*609 (95 cm^{-1}). In domain 3 (with *a*604, *b*606, and *b*607 chromophores), the coupling matrix element between *a*604−*b*607 and *b*607−*b*606 is moderate, i.e., ∼33 and ∼30 cm^{-1}, respectively (see Table A1 in the Appendix), but the coupling between *a*604 and *b*606 is strong, that is, 91 cm^{-1}. In summary, compared to the previous structural model,[13] the X-ray structure revealed five more pigments: *a*604, *b*607, *b*608, *a*611, and *a*615, whose names are marked with black panes in Figure 1A. Note that the CP29 structure[12] is very similar to that of the major LHCII antenna complex of PSII,[17] with 14 chromophores, whose pigment labeling is given in the left column for comparison. Labeling of pigments in CP29 based on ref 13 is shown in the right column for easy comparison.

It has been argued in recent years that the CP29 complex plays an important physiological role in the PSII supercomplexes.[2] That is, besides the main function of light-harvesting, CP29 stabilizes the whole PSII supercomplex[2] and is responsible for transferring energy from LHCII and CP24 to the PSII RC. This makes CP29 a very suitable site for regulation of the excitation energy flow, i.e., photoprotection.[18−20] However, there is no agreement on which pigment(s) contributes to the lowest energy state(s) in CP29; based on the analogy with the LHCII protein, the likely candidates include the *a*612−*a*611−*a*610 trimer and/or *a*603−*a*609 dimer within the *a*603−*a*609−*b*608 cluster,[12] although a contribution from Chl *a*604 in the *a*604−*b*606−*b*607 cluster in spinach CP29 cannot be excluded,[21] as reconstituted complexes did not possess this pigment.[16] Note that the Lut−*a*612−*a*611−*a*610 cluster in CP29 is similar to the Lut−*a*610−*a*612−*a*611 present in LHCII, which acts as the energy exit in LHCII.[22−25] Recent site directed mutagenesis studies suggested that Chl *a*612 contributes to the low-energy states at room temperature.[26] Below, we report various experimental and calculated (low-temperature) spectra, including HB and CD spectra, to provide more insight into excitonic structure and EET in the CP29 protein complex. We focus on the following questions: (1) which cofactors contribute to the lowest energy state(s), (2) what is the composition of the low-energy exciton state(s), and (3) which cluster of pigments serves as a potential energy-quenching center and/or as the exit or entrance in energy transfer pathways.

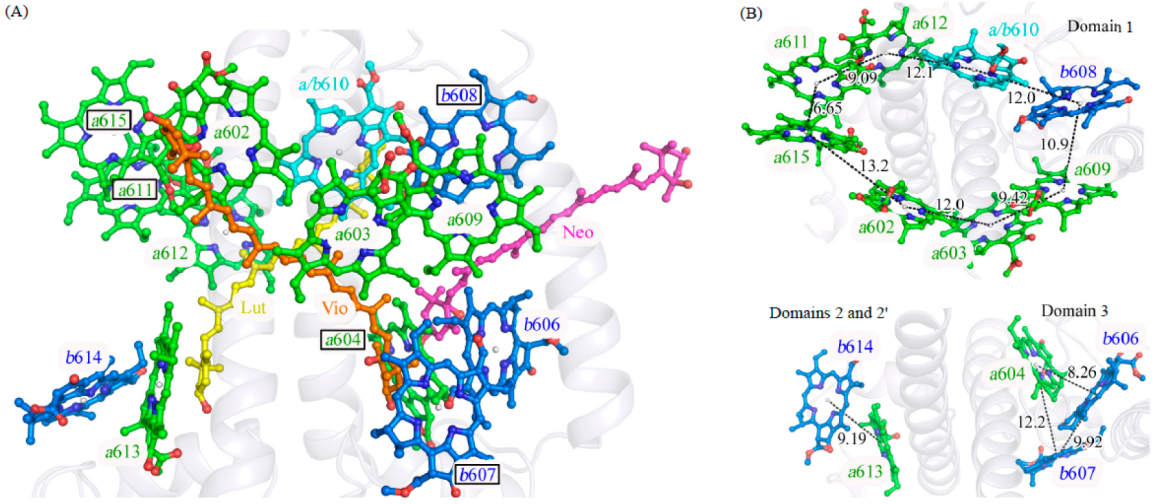

Figure 1. (A) Pigment arrangement in CP29. View along the membrane plane. For clarity, the Chl phytyl chains are not shown. Green, Chl *a*; blue, Chl *b*; cyan, mixture binding site Chl *a*/*b*610; yellow, Lut; orange, Vio; magenta, Neo. Chl's that could not be identified in the predicted model based on the reconstituted CP29 are marked with black rectangles. (B) All the pigments are shown in domains: Chl's in the stromal layer (domain 1), Chl's in the luminal layer (domains 2/2′ and 3). The adjacent Chl's in each layer are connected with black dashed lines, and the distances (Å) of their central Mg atoms are labeled with black numbers.

dx.doi.org/10.1021/jp4004328 | J. Phys. Chem. B XXXX, XXX, XXX−XXX

2. MATERIALS AND METHODS

2.1. Isolation and Purification of CP29. The sample was prepared in the same procedure as ref 12. Briefly, spinach PSII membrane fragments were isolated as described previously[27] and were washed using 400 mM sucrose, 5 mM $MgCl_2$, 15 mM NaCl, and 50 mM Mes (pH 6.5) to remove excess Triton X-100. Extrinsic and some hydrophobic polypeptides were removed from the PSII particles by incubation in 0.8 M Tris/HCl (pH 8.35) at a chlorophyll concentration of 0.2 mg/mL, under room illumination and on ice for 30 min. The Tris-treated PSII was resuspended in 10 mM MES pH 6.0 and solubilized in 2% Sulfobetaine 12 (SB-12) and 1% *n*-dodecyl-*β*-maltoside (*β*-DDM) with the final Chl concentration at 2 mg/mL and then stirred on ice for 30 min. After centrifugation at 40000*g* for 30 min, the supernatant was loaded on to the weak cation exchange column Hiprep 16/10 CM FF (GE healthcare) to remove contamination from the other PSII antenna proteins. The buffer was 0.1% (w/v) SB-12 and 0.03% (w/v) *β*-DDM, 10 mM MES, pH 6.0, 0.02% NaN_3 with 0−0.5 M NaCl gradient. The eluted fractions were concentrated and loaded for size exclusion chromatography (Superdex 200 16/300 GL column, GE Healthcare) to improve sample homogeneity. The buffer for size exclusion chromatography contained 20 mM sodium HEPES, pH 7.5, 1.5% (w/v) *n*-heptyl-*β*-D-thioglucopyranoside (HTG, Anatrace), and 0.02% (w/v) NaN_3. The Chl *a*/*b* ratio of CP29 protein solution used in our studies was around 2.3 ± 0.1, and was obtained using the methodology of Porra et al.[28]

2.2. Experimental Setup. Details about the measurement setup were described elsewhere.[29] Here, only a brief description is given. A Bruker HR125 Fourier transform spectrometer was used to measure the absorption and HB spectra. In absorption and nonresonant HB, the resolution was set at 4 cm^{-1}. For resonant HB, spectral resolution of 1 cm^{-1} was used. The fluorescence spectra were collected by a Princeton Instruments Acton SP-2300 spectrograph equipped with a back-illuminated CCD camera (PI Acton Spec-10, 1340 × 400). All emission spectra were obtained with a resolution of 0.1 nm. The laser source for both nonresonant HB and fluorescence was 496.5 nm, produced from a Coherent Innova 200 argon ion laser. The optical density (OD) of the sample for the nonresonant HB, resonant HB, and emission spectra was 0.8, 1.5, and 0.1, respectively. In the resonant HB experiments, the tunable wavelengths came from a Coherent CR699 ring dye laser pumped by a Millenia 10s diode-pumped, solid-state laser at 532 nm from Spectra-Physics. With laser dye LD 688 (Exciton), the spectral range of 650−720 nm was available with a line width of 0.07 cm^{-1}. Power from the ring laser output was stabilized with a Laser Power Controller (Brockton Electro-Optics Corp.). Laser power in the experiments was precisely set by a continuously adjustable neutral density filter. All experiments were performed at 5 K inside a Janis 8-DT Super Vari-Temp liquid helium cryostat. Sample temperature was read and controlled with a Lakeshore Cryotronic model 330 temperature controller. To minimize aggregation of the CP29 complexes, 0.03% *β*-DDM was added to the original buffer of 2.0% HTG, 10 mM MES, and pH 6.5.

3. RESULTS

3.1. Experimental Absorption and Emission Spectra. Normalized 5 K absorption (curve a) and emission (curve a′) spectra of the CP29 antenna protein complex obtained in this work are shown in Figure 2. The emission spectrum was measured with a total fluence of ∼70 mJ/cm^2 to minimize hole burning (HB). The 4.2 K absorption (curve b) and emission (curve b′) spectra from ref 30 are shown for comparison. In the Chl *a* region, the absorption spectrum (curve a) exhibited a prominent band at 674.8 nm and a shoulder near 670 nm. The two bands near 638.9 and 650.4 nm were due to Chl *b* molecules of CP29.[31] Compared with the absorption spectrum of Pieper et al.,[30] all three peaks were slightly broader and red-shifted by 0.2−0.4 nm. The most striking difference was that our CP29 sample (when arbitrarily normalized at absorption maximum) has (i) a larger bandwidth in the Chl *a* Q_y-absorption region with a band maximum at 674.8 nm, (ii) a more prominent shoulder near 665−670 nm, and (iii) a relatively stronger absorbance due to Chl *b* molecules near 650 nm. That is, the main absorption bands in curves a and b had a full width at half-maximum (fwhm) of 300 and 233 cm^{-1}, respectively. The emission spectrum (curve a′) had a maximum at 680.0 nm (with a fwhm of 174 cm^{-1}), which is about 0.7 nm red-shifted in peak position and 14 cm^{-1} broader (when compared to the emission spectrum reported previously in ref 30), as shown by curve b′. Both emission spectra had very similar vibronic regions with the major peaks around 715 and 740 nm. A contribution from aggregated CP29 complexes must be minor, as the emission spectrum of aggregated CP29 complexes (see curve c′) had a maximum near 690 nm and was significantly broader (fwhm = 444 cm^{-1}). Aggregated complexes were prepared with a significantly decreased concentration of detergent.

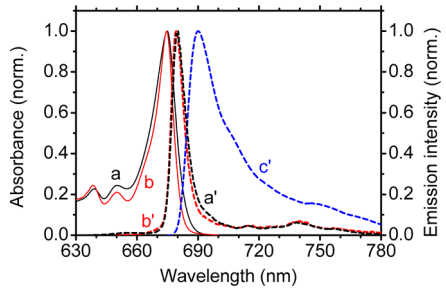

Figure 2. Curves a/b and a′/b′ (normalized on peak intensities) correspond to the 5/4.2 K absorption and fluorescence spectra of CP29 studied in this work and ref 28, respectively. Curve c′ represents the emission spectrum of the aggregated CP29 sample (this work).

3.2. Nonresonant HB Spectra. Figure 3 shows the HB (nonresonant) spectra (T = 5 K) of CP29 obtained at different burn fluence with a burn wavelength (λ_B) of 496.5 nm. The shallowest and saturated holes (curves a and i) were burned with a fluence ($f = I{\cdot}t$) of 6 J/cm^2 (I = 600 mW/cm^2 for t = 10 s) and 7 kJ/cm^2 (I = 600 mW/cm^2 for t ∼ 12,000 s), respectively. With increasing burn fluence, the main hole position shifted from 679.7 nm (curve a) to 678.8 nm (curve i), as illustrated in the inset of Figure 3. Interestingly, there was also a small hole at ∼640 nm whose relative intensity at highest fluence was smaller by a factor of 20 when compared with the main holes near 679−680 nm.

Note the above fluence dependent position of our saturated 678.8 nm hole is similar to that observed in ref 30, although the holes are broader and slightly red-shifted. This is an indication that the CP29 complex studied previously had a different composition of low-energy state(s).

dx.doi.org/10.1021/jp4004328 | J. Phys. Chem. B XXXX, XXX, XXX−XXX

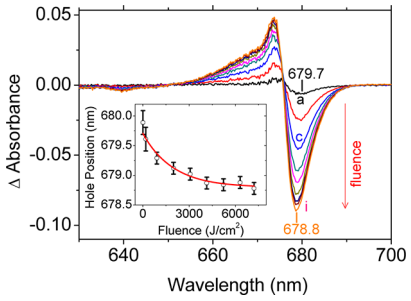

Figure 3. HB spectra of CP29 (T = 5 K) obtained with different burn fluence and excitation wavelength of 496.5 nm. Hole positions for the shallow (curve a) and saturated holes (curve i) are at 679.7 and 678.8 nm, respectively. The inset shows the broad hole position as a function of the burn fluence.

The HB spectrum obtained with λ_B = 665.0 nm (curve a; resolution 1 cm^{-1}) is compared in Figure 4 with the HB

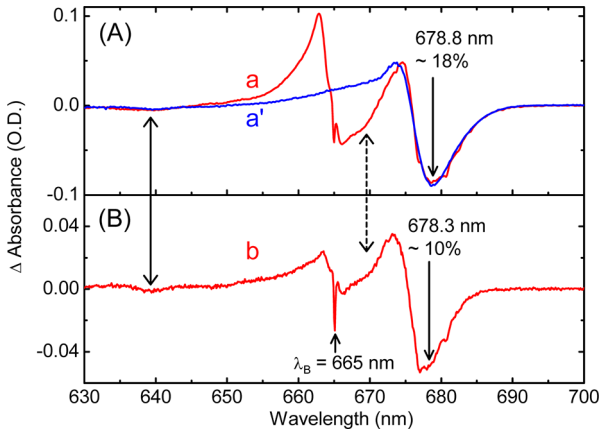

Figure 4. (A) Curves a and a′ are the HB spectra of the CP29 complex (this work) obtained with λ_B = 665.0 and 496.5 nm, respectively. (B) HB spectrum obtained with λ_B = 665.0 nm and adopted from ref 23. See text for details.

spectrum measured with λ_B = 496.5 nm (curve a′, identical to curve i in Figure 3). Curve b in frame B of Figure 4 (λ_B = 665.0 nm; shown only for comparison with spectrum a) is from ref 30. All HB spectra shown in Figure 4 are saturated or nearly saturated. Comparing curves a and a′ (without any normalization), one can see the two main holes at 678.8 nm match very well concerning the position and shape of the lowest energy band. However, as mentioned above (see also Figure 3), spectra a and a′ each have a very shallow satellite hole around 640 nm, which is relatively deeper in curve b in Figure 4B. These data further indicate that the samples discussed in this work have different types of Chl contributing to the lowest energy state(s). Different hole depths near 670 nm, marked with a dashed double arrow in Figure 4B, further support the possibility that CP29 studied in ref 30 contained a smaller number of pigments.

In summary, comparison of curves a and b in Figure 4 reveals three major differences: (1) the saturated hole in curve a is much deeper (18%) than that in curve b (10%) from ref 30; (2) spectrum a, burned at 665.0 nm, reveals a much deeper hole around 670 nm, as indicated by a dashed double arrow; (3) the main bleach in curve b is narrower and slightly blue-shifted in comparison with spectra a/a′; and (4) the satellite hole around 639 nm (indicated by a solid double arrow) is relatively deeper in curve b (frame B) than that revealed in curves a/a′. Note that the hole depth (in %) corresponds to the ratio between the Δ absorbance of the hole and the absorbance at the wavelength corresponding to the hole minimum. The absence of correlation between the 678.8 and ~639 nm bleaches is discussed in section 4.4.

3.3. Resonant HB Spectra. Figure 5A shows the resonant HB spectrum obtained with λ_B = 638.5 nm (black noisy curve),

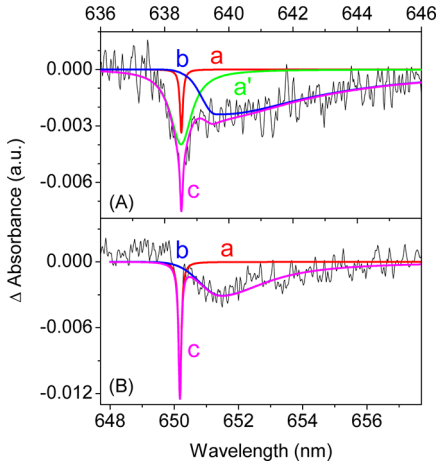

Figure 5. (A) Resonant HB spectrum (noisy curve) of CP29 at 5 K with λ_B = 638.5 nm. The spectrum was fitted with two Lorentzian ZPLs (curves a and a′) and one combined PSB (curve b). Curve c is the sum of curves a, a′, and b. The fwhm of the ZPHs (curves a and a′) are 2.5 and 23 cm^{-1}, respectively. The pseudo-PSB hole (curve b) is a half Gaussian/half Lorentzian with an fwhm of 26/150 cm^{-1}. (B) Fit of the resonant HB spectrum (λ_B = 650.2 nm) of CP29 (noisy curve) at 5 K with fits of the ZPH and PSB, curves a and b, respectively. Curve c is the sum of curves a and b. The fwhm of the ZPH (curve a) is 2.5 cm^{-1}. The pseudo-PSB hole (curve b) is a half Gaussian/half Lorentzian with an fwhm of 30/82 cm^{-1}.

burned in the absorption band contributed to by Chl *b* molecules. The HB spectrum can be fitted with two Lorentzians, a and a′, of different widths (zero-phonon holes, ZPHs), and their combined phonon sideband (PSB) hole, curve b, which is half Gaussian on the high-energy side and half Lorentzian on the low-energy side, a shape typically observed in HB spectra.[32−34] The fwhm of curves a and a′ are 2.5 and 23 cm^{-1}, respectively. Using $T_1 = (\pi c \Gamma_{hole})^{-1}$, where c is the speed of light and Γ_{hole} is the Lorentzian hole width, one obtains lifetimes of 4.0 ± 0.7 and 0.4 ± 0.1 ps, respectively. The pseudo-PSB hole (curve c) is a half Gaussian/half Lorentzian with a fwhm of 26/150 cm^{-1}.

The resonant HB spectrum with λ_B = 650.2 nm (shown in Figure 5B) can be perfectly fitted with one component; in the fit, the ZPH (curve a) has an fwhm of 2.5 cm^{-1}. The broad hole with a minimum peaking at ~28 cm^{-1} from the ZPH reflects the shape of the pseudo-PSB hole. In this case, the pseudo-PSB hole (curve c) can be described as half Gaussian/half Lorentzian with a fwhm of 30/82 cm^{-1}, respectively. From the ZPH width, the depopulation of the excited state of Chl *b* absorbing near 650 nm is 4.0 ± 0.7 ps.

4. DISCUSSION

As outlined in the Introduction section, the recent X-ray structure[12] revealed five more pigments present in the CP29

dx.doi.org/10.1021/jp4004328 | J. Phys. Chem. B XXXX, XXX, XXX−XXX

complex from spinach than previously believed,[13] i.e., 13 pigments in total. However, a smaller number of pigments (eight in total[13]) observed in reconstituted CP29 complexes (i.e., six Chl *a* and two Chl *b* molecules per CP29 monomer) does not have to apply to the WT CP29 antenna isolated from spinach. In addition, it is feasible that some Chl's could be lost during purification procedures. Since proteins used in this study were used in a recent structural determination, we assume our CP29 complexes contain 13 pigments, as revealed by X-ray data.[12] This number is similar to the LHCII antenna complex where 14 pigments were observed.[17] We argue below that the larger number of Chl's in our preparation is consistent with several types of optical spectra reported in this work and modeling studies reported in part II (DOI 10.1021/jp4004278). We focus below on the differences observed in absorption and HB spectra near 640, 670, and 680 nm. More insight into the HB spectra (including antihole) whose shape is sensitive to the excitonic structure of the CP29 complex, especially the composition of the lowest exciton state(s), is provided in part II (DOI 10.1021/jp4004278).

4.1. More on Absorption and Emission Spectra. Figure 2 clearly indicates the integrated absorption intensity of curve a (for arbitrarily normalized spectra at the absorption maximum) is larger than that represented by spectrum b adopted from ref 30. In the first approximation, based on the comparison of the integrated areas of spectra a and b in Figure 2, it appears the CP29 sample represented by curve b likely contains a smaller number of pigments that must have been lost during the isolation/purification procedure. The difference between the integrated areas in the Q_y spectral region of spectra a and b is ~1.7 in Chl *a* units. However, since the two spectra are *normalized arbitrarily* at the maximum of the Q_y band, the area difference does not necessarily mean the pigment number difference is ~1.7 in the two samples, as the number difference depends on normalization. We want to emphasize that the slightly broader and red-shifted fluorescence origin band (curve a′ in Figure 2) is not due to aggregation phenomena, although a very small contribution near 690 nm from aggregated complexes cannot be excluded, as emission from aggregated complexes peaks near 690 nm. Interestingly, Rätsep et al.[35] observed that conventional FLN spectra, excited at 678 and 680 nm, were composed of more than one emitter, which were also differently affected by HB. It is feasible the presence of two subpopulations of CP29, with slightly different composition of the low-energy states, could be responsible for this behavior. That is, it cannot be excluded that the previously studied CP29 samples consisted of complexes with different numbers of pigments, i.e., complexes with a different composition of the low-energy fluorescent state (*vide infra*).

Now let us look at the site energies of these Chl molecules. It is well-known[31] that the two peaks around 638.9 and 650.4 nm belong to Chl *b* molecules, but their identification (i.e., an association with a particular absorption band) was not determined. The best fits of the above spectra (for details, see the accompanying paper) indicated that the 638.9 and 650.4 nm absorption bands are contributed to by the *b*608/*b*614 and *b*606/*b*607 chromophores, respectively. Here, we only mention that the site energies of *b*608/*b*614 and *b*606/*b*607 are 15700/15740 and 15410/15410 cm^{-1}, respectively. As for the Chl *a* molecules, based on simultaneous modeling of the above spectra, the lowest site energies were assigned to *a*612 (14940 cm^{-1}; 669.3 nm), *a*611 (15000 cm^{-1}; 666.7 nm), and *a*610 (14990 cm^{-1}; 667.1 nm). These pigments, especially *a*612 and *a*611, contribute most strongly to the lowest energy exciton state in the intact CP29 protein, constituting the exit trap in energy-transfer pathways at low temperatures. More details on simulations using the Redfield-based approach and the composition of all exciton states are discussed in the accompanying paper (part II, DOI 10.1021/jp4004278).

4.2. Sample-Dependent Shape of Nonresonant HB Spectra. Different pigment composition in the CP29 samples discussed above is further supported by comparison of the 665.0 nm burned nonresonant HB spectra replotted in Figure 6.

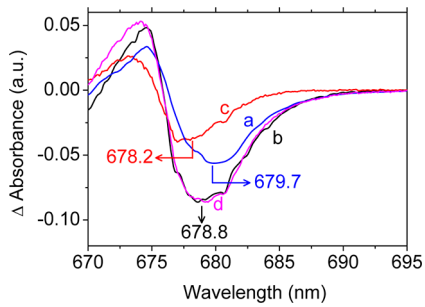

Figure 6. Nonresonant HB spectra of CP29 obtained for two different preparations from spinach. Curves a and b (T = 5 K) are the shallow (blue) and saturated (black) holes obtained for the sample studied in this work, respectively. Curve c (T = 4.2 K), shown for comparison, is the saturated hole from ref 30. Curves a and c are normalized in such a way that their sum (curve d) matches curve b.

Here, the shallow (~1.5%) and saturated (~18%) holes from this work (spectra a and b, respectively, in Figure 6; not scaled for the hole depth) are compared with the scaled saturated HB (~10%) spectrum from ref 30 (curve c). The shallow (low-fluence) hole is centered at ~679.7 nm (curve a). This broad hole shifts to the blue with higher burning fluence, as illustrated in Figure 3. Note that hole i in Figure 3 ($f \sim 7$ kJ/cm^2) is nearly saturated (see the corresponding inset) and shifted blue to about 678.8 nm. That is, the second lowest energy state that comes into play after the lowest energy state is non-photochemically burned and, as a result, ceases to be the lowest state. This leads to the blue-shift of the nonresonant HB spectra, as illustrated in Figure 3.

The comparison shown in Figure 6 is only for illustrative purposes, as the number of pigments in CP29 studied in ref 30 is unknown, and the fluence dependence of the nonresonant HB spectra is different in these two samples (*vide supra*). That is, in contrast to the behavior shown in Figure 3, the nonresonant holes, as discussed by Pieper et al.,[30] did not shift as a function of fluence. It was for that reason the authors concluded that the lowest energy state in their CP29 sample was likely localized on a single Chl *a* molecule. The blue-shift of our nonresonant HB spectrum clearly suggests that our sample has a different composition of the lowest energy state(s). The fact that the sum of our shallow (low-fluence) hole and the saturated hole from ref 30 (spectrum c), plotted as curve d = a + c, is similar to our saturated HB spectrum (curve b) is likely accidental, as due to a different number of pigments the composition of the lowest energy states must differ (see the accompanying paper, DOI 10.1021/jp4004278).

Regarding the broad nonresonant (i.e., non-line-narrowed) holes shown in Figure 3, we suggest these blue-shifted holes (curves a–i) are contributed to by the second lowest energy state that comes into play after the lowest energy state is

dx.doi.org/10.1021/jp4004328 | J. Phys. Chem. B XXXX, XXX, XXX–XXX

non-photochemically burned (and ceases to be the lowest state). This leads to a blue-shift of the HB spectra shown in Figure 3, as already observed in several pigment antenna complexes.[29,36] Furthermore, this assignment is consistent with modeling studies using the Redfield approach, as further discussed in the accompanying paper (part II, DOI 10.1021/jp4004278). Here, we only note that the saturated hole near 678.8 nm (curve b in Figure 6) can be contributed by more than one exciton state.

Comparison of the integrated intensities of the absorption and nonresonant HB spectra (not shown for brevity) revealed that the oscillator strength of the lowest energy state is equivalent to about one Chl *a*. This does not mean, however, that the lowest energy state is necessarily localized on a single Chl *a* molecule, since the CP29 preparations discussed in this work showed different behavior of the corresponding lowest energy states. A possible explanation (further discussed in part II, DOI 10.1021/jp4004278) is that the previously studied CP29 complexes lost one or two Chl's, contributing partly to the lowest energy state. The most likely candidate is the externally located *a*615−*a*611 pair, which shares a molecule of glycerol-3-phosphate or phospholipid as their central ligand. These Chl's could be lost during the isolation/purification procedure, leading to a blue-shifted low-energy exciton state and different behaviors as a function of fluence.

4.3. On Possible Correlation of the ∼680 and ∼640 nm Bleaching. In Figure 7, we inspect the relative ratio of holes

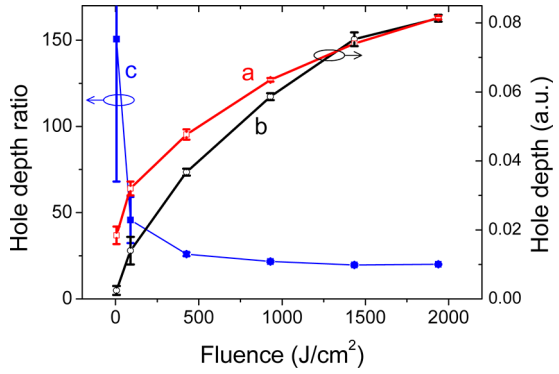

Figure 7. Depths of the main hole at ∼679 nm from Figure 3 (red curve a), its satellite hole at ∼640 nm (curve b, magnified by 20), and their ratio (curve c) plotted as a function of the burn fluence (f).

near 680 and 640 nm presented in Figure 3. Here, we plot the depths of the above two holes and their ratio as a function of the burn fluence (f). It appears that at the early stage of burning (f < 100 J/cm^2) the ratio clearly changes, indicating these two holes burned at 496.5 nm are not correlated. This is why the hole depth of the ∼640 nm holes obtained for λ_B = 665.0 nm in two different CP29 (see Figure 4, spectra a and b) is sample dependent. Since there is no ∼640 nm bleach in the calculated NPHB spectra (see the accompanying paper, DOI 10.1021/jp4004278), we conclude that this bleach is not an excitonic satellite hole of the main hole bleached near 680 nm (this work) and/or near 679 nm in ref 30, but it is produced via conformational changes of the protein produced by HB of the Chl *a* molecules associated with the lowest energy state. The possibility of a conformational change has been mentioned in ref 30 for the LHCII complex. Conformational changes might be spatially extended in a way that they affect the transition frequency of one or two Chl *b* molecules in the vicinity of the lowest energy state; here the most likely candidate is the Chl *b* in the mixed-binding site *a*/*b*610 and/or Chl *b*608 (with site energies near 640 nm) that are located in the vicinity of the lowest energy state. The latter is consistent with our excitonic calculations (see part II, DOI 10.1021/jp4004278), where we show the lowest energy state in CP29 is mostly contributed to by the *a*612−*a*611 Chl pair (57%), Chl *a*615 (12%), and *a*610 (11%). Note that the Mg−Mg distance of *b*608−*a*/*b*610 in CP29 is only 12 Å, which is similar to the Mg−Mg distance between *b*608 and *a*610 Chl's in LHCII (11.7 Å).[17] In addition, it is feasible that conformational changes mentioned above could be more strongly manifested in proteins that lost some pigments during preparation/purification procedures.

4.4. Depopulation of the Excited States Probed at λ_B via Chl *b* → Chl *a* and Chl *a* → Chl *a* Excitation Energy Transfer. From data presented in Figure 5, depopulation lifetimes can be obtained, using $T_1 = (\pi c \Gamma_{hole})^{-1}$, where c is the speed of light and Γ_{hole} is the Lorentzian hole width. From data shown in Figure 5A (λ_B = 638.5 nm), one obtains lifetimes of 0.4 ± 0.1 and 4 ± 0.7 ps. The fast lifetime of ∼0.4 ps most probably represents the depopulation of the excited states probed at λ_B via *b*608 → *a*603−*a*609 dimer (note, the nearest Chl *a* in the vicinity of *b*608 is *a*609). The distance of their center Mg atoms is 10.9 Å in domain 1. The slower component of ∼4 ps most likely corresponds to EET from domain 2′ to domain 1. Our lifetimes of ∼4 and ∼0.4 ps are about 2 times slower than the two fastest components observed at 77 K in species-associated difference spectra (SADS), i.e., 2.2 and 0.22 ps in ref 37. This suggests that complexes studied by Gradinaru et al. possessed both Chl's *b*614 and *b*608. Note that the fast component of 0.6 ps was also reported for the LHCII complex (i.e., Chl *b* → Chl *a*) at room temperature.[38] A lifetime of 0.35 ± 0.05 ps was also observed in CP29 for the "blue" Chl *b* (absorption around 640 nm) at 77 K in ref 39. Interestingly, the resonant HB spectrum burned at ∼640 nm in the previously studied CP29 complexes[30] was fitted by one Lorentzian, which gave a lifetime of 0.90 ± 0.15 ps at 5 K, suggesting that this lifetime may be the average of two nonresolved lifetime components. From the ZPH width, the depopulation of the excited state of Chl *b* absorbing near 650 nm (likely contributed to by *b*606 and *b*607 in domain 3) is 4.0 ± 0.7 ps. However, this time could simply reflect the EET from domain 3 to domain 1. This EET time is comparable with the value of 4.2 ± 0.3 ps measured at 5 K in ref 30, suggesting that both Chl's *b*606 and *b*607 were present in our preparation and in the CP29 proteins studied in ref 30, or one of those Chl's was absent in both preparations (see part II (DOI 10.1021/jp4004278), where we argue that Chl *b*607 was lost in both samples). Therefore, we propose that a subpopulation of CP29 studied in ref 30 could be, in part, depleted of Chl *b*607 (domain 3), whose absence, along with the absence of *a*615 or *a*611, would modify the EET dynamics and electronic spectra (including HB spectra) in qualitative agreement with our experimental observations. A smaller lifetime of 2.2 ± 0.5 ps was also observed in CP29 for the "red" Chl *b* (absorption around 650 nm) at 77 K in ref 39.

5. CONCLUDING REMARKS

Low-temperature, laser-based spectroscopy was used to investigate an excitonic structure and EET processes in the CP29 complex isolated from spinach. On the basis of the comparison with published absorption, emission, and HB spectra of CP29,[30] we suggest that previously studied samples contained a large subpopulation of complexes with a smaller number of

pigments, which could have been lost during the preparation/isolation procedure. We propose that the two lowest energy exciton states are strongly delocalized with the most likely contribution from the *a*612−*a*611−*a*615−*a*610 cluster in domain 1. This is in agreement with the LHCII complex, where the trimer *a*610−*a*612−*a*611 was identified as the lowest energy state. We believe that spectral differences observed between the samples studied in ref 30 and the sample investigated in this work could be explained assuming the former preparation did not contain *a*615 or *a*611 and likely *b*607 Chl molecules. The latter would lead to the experimentally observed blue-shift in absorption/emission spectra in ref 30. The absence of the fast component (∼0.4 ps) observed in our CP29 complex and in ref 37, which most probably represents the depopulation of the excited states probed at λ_B = 638.2 nm via *b*608 → *a*603−*a*609 dimer in domain 1, suggests that the lifetime of 0.90 ± 0.15 ps at 5 K reported in ref 30 most likely represented the average of two nonresolved lifetime components observed in our CP29 sample. In summary, we conclude that the *a*612−*a*611−*a*615−*a*610 cluster contributes mostly to the lowest energy state in CP29 and could likely serve as the exit state in energy-transfer pathways at physiological temperatures.

APPENDIX

Table A1. Coupling Matrix Elements (V_{nm} in cm^{-1}) between 13 Chl's in the CP29 Protein (Assuming That the Mixed Site Is Occupied by Chl *a*610)[a]

	*a*603	*a*604	*b*606	*b*607	*b*608	*a*609	*a*610	*a*611	*a*612	*a*613	*b*614	*a*615
*a*602	23	8	7	9	−9	−36	−8	0	12	−3	0	51
*a*603		−1	−5	7	6	95	10	−1	1	3	−5	−3
*a*604			91	33	−6	−5	−3	−4	2	3	−3	−4
*b*606				30	−7	3	−2	−3	2	2	−2	−3
*b*607					−5	−10	0	−3	3	4	−2	−3
*b*608						37	53	6	−1	−3	1	7
*a*609							−2	5	−1	−4	2	8
*a*610								−41	22	8	0	−11
*a*611									86	−5	2	96
*a*612										1	0	−2
*a*613											−6	−6
*b*614												1

[a]The calculation is based on the PDB 3PL9 structure[12] using the TrEsp method from ref 40. Effective dipole strengths of 18.5 and 13 D^2 are used for Chl *a* and Chl *b* molecules, respectively.

AUTHOR INFORMATION

Corresponding Author

*E-mail: ryszard@ksu.edu.

Notes

The authors declare no competing financial interest.

[⊥]R.J.: On a sabbatical leave from Kansas State University, Manhattan, Kansas 66506.

ACKNOWLEDGMENTS

This work was supported by the NSF ARRA Grant (CHE-0907958) to R.J. The authors are thankful to Mukund Koirala (K-State) for experimental help during the early stages of this work. We also acknowledge Mike Reppert (Cambridge, MIT) and Adam Kell (K-State) for fruitful discussions and Dr. Zhenfeng Liu for help during the work. CP29 complexes were prepared in Prof. Wenrui Chang's laboratory (supported by the 973 Project 2011CBA00902 to W.C.). J.P. gratefully acknowledges support by the European Social Fund's Internationalisation Programme DoRa, by Estonian Science Foundation (Grant No 9453), and Estonian Institutional Grant TLOFY 13028I.

REFERENCES

(1) Dekker, J. P.; Boekema, E. J. *Biochim. Biophys. Acta* **2005**, *1706*, 12−39.
(2) Caffarri, S.; Kouril, R.; Kereiche, S.; Boekema, E. J.; Croce, R. *EMBO J.* **2009**, *28*, 3052−3063.
(3) Novoderezhkin, V. I.; van Grondelle, R. *Phys. Chem. Chem. Phys.* **2010**, *12*, 7352−7365.
(4) van Grondelle, R.; Novoderezhkin, V. I. *Phys. Chem. Chem. Phys.* **2006**, *8*, 793−807.
(5) Croce, R.; van Amerongen, H. *J. Photochem. Photobiol., B* **2011**, *104*, 142−153.
(6) Loll, B.; Kern, J.; Saenger, W.; Zouni, A.; Biesiadka, J. *Nature* **2005**, *438*, 1040−1044.
(7) Guskov, A.; Kern, J.; Gabdulkhakov, A.; Broser, M.; Zouni, A.; Saenger, W. *Nat. Struct. Mol. Biol.* **2005**, *16*, 334−342.
(8) Caffarri, S.; Croce, R.; Cattivelli, L.; Bassi, R. *Biochemistry* **2004**, *43*, 9467−9476.
(9) Camm, E. L.; Green, B. R. *Plant Physiol.* **1980**, *66*, 428−432.
(10) Jansson, S. *Trends Plant Sci.* **1999**, *4*, 236−240.
(11) Dainese, P.; Bassi, R. *J. Biol. Chem.* **1991**, *266*, 8136−8142.
(12) Pan, X.; Li, M.; Wan, T.; Wang, L.; Jia, C.; Hou, Z.; Zhao, X.; Zhang, J.; Chang, W. *Nat. Struct. Mol. Biol.* **2011**, *18*, 309−315.
(13) Bassi, R.; Croce, R.; Cugini, D.; Sandona, D. *Proc. Natl. Acad. Sci. U.S.A.* **1999**, *96*, 10056−10061.
(14) Caffarri, S.; Passarini, F.; Bassi, R.; Croce, R. *FEBS Lett.* **2007**, *581*, 4704−4710.
(15) Gastaldelli, M.; Canino, G.; Croce, R.; Bassi, R. *J. Biol. Chem.* **2003**, *278*, 19190−19198.
(16) Giuffra, E.; Zucchelli, G.; Sandona, D.; Croce, R.; Cugini, D.; Garlaschi, F. M.; Bassi, R.; Jennings, R. C. *Biochemistry* **1997**, *36*, 12984−12993.
(17) Liu, Z.; Yan, H.; Wang, K.; Kuang, T.; Zhang, J.; Gui, L.; An, X.; Chang, W. *Nature* **2004**, *428*, 287−292.
(18) Ahn, T. K.; Avenson, T. J.; Ballottari, M.; Cheng, Y.-C.; Niyogi, K. K.; Bassi, R.; Fleming, G. R. *Science* **2008**, *320*, 794−797.
(19) Betterle, N.; Ballottari, M.; Zorzan, S.; de Bianchi, S.; Cazzaniga, S.; Dall'Osto, L.; Morosinoto, T.; Bassi, R. *J. Biol. Chem.* **2009**, *284*, 15255−15266.
(20) Mozzo, M.; Passarini, F.; Bassi, R.; van Amerongen, H.; Croce, R. *Biochim. Biophys. Acta* **2008**, *1777*, 1263−1267.
(21) Pieper, J.; Rätsep, M.; Irrgang, K.-D.; Freiberg, A. *J. Phys. Chem. B* **2009**, *113*, 10870.
(22) Ruban, A. V.; Berera, R.; Ilioaia, C.; van Stokkum, I. H. M.; Kennis, J. T. M.; Pascal, A. A.; van Amerongen, H.; Robert, B.; Horton, P.; van Grondelle, R. *Nature* **2007**, *450*, 575−578.
(23) Remelli, R.; Varotto, C.; Sandonà, D.; Croce, R.; Bassi, R. *J. Biol. Chem.* **1999**, *274*, 33510−33521.
(24) Rogl, H.; Schödel, R.; Lokstein, H.; Kühlbrandt, W.; Schubert, A. *Biochemistry* **2002**, *41*, 2281−2287.
(25) Novoderezhkin, V. I.; Palacios, M. A.; van Amerongen, H.; van Grondelle, R. *J. Phys. Chem. B* **2005**, *109*, 10493−10504.
(26) Belgio, E.; Casazza, A. P.; Zucchelli, G.; Garlaschi, F. M.; Jennings, R. C. *Biochemistry* **2012**, *49*, 882−892.
(27) Berthold, D. A.; Babcock, G. T.; Yocum, C. F. *FEBS Lett.* **1981**, *134*, 231−234.
(28) Porra, R. J.; Thompson, W. A.; Kriedemann, P. E. *Biochim. Biophys. Acta* **1989**, *975*, 384−394.
(29) Feng, X.; Neupane, B.; Acharya, K.; Zazubovich, V.; Picorel, R.; Seibert, M.; Jankowiak, R. *J. Phys. Chem. B* **2011**, *115*, 13339−13349.

(30) Pieper, J.; Irrgang, K.-D.; Rätsep, M.; Voigt, J.; Renger, G.; Small, G. *J. Photochem. Photobiol.* **2000**, *71*, 574−581.
(31) Pascal, A.; Gradinaru, C.; Wacker, U.; Peterman, E.; Calkoen, F.; Irrgang, K.-D.; Horton, P.; Renger, G.; van Grondelle, R.; Robert, B.; van Amerongen, H. *Eur. J. Biochem.* **1999**, *262*, 817−823.
(32) Jankowiak, R.; Reppert, M.; Zazubovich, V.; Pieper, J.; Reinot, T. *Chem. Rev.* **2011**, *111*, 4546−4598.
(33) Jankowiak, R.; Hayes, J. M.; Small, G. J. *Chem. Rev.* **1993**, *93*, 1471−1502.
(34) Völker, S. *Annu. Rev. Phys. Chem.* **1989**, *40*, 499−530.
(35) Rätsep, M.; Pieper, J.; Irrgang, K.-D.; Freiberg, A. *J. Phys. Chem. B* **2008**, *112*, 110−118.
(36) Neupane, B.; Dang, N. C.; Acharya, K.; Reppert, M.; Zazubovich, V.; Ricorel, R.; Seibert, M.; Jankowiak, R. *J. Am. Chem. Soc.* **2010**, *132*, 4214−4229.
(37) Gradinaru, C. C.; van Stokkum, I. H. M.; Pascal, A. A.; van Grondelle, R.; van Amerongen, H. *J. Phys. Chem. B* **2000**, *104*, 9330−9342.
(38) Bittner, T.; Wiederrecht, G. P.; Irrgang, K. D.; Renger, G.; Wasielewski, M. *Chem. Phys.* **1995**, *194*, 311−322.
(39) Gradinaru, C. C.; Pascal, A. A.; van Mourik, F.; Robert, B.; Horton, P.; van Grondelle, R.; van Amerongen, H. *Biochemistry* **1998**, *37*, 1143−1149.
(40) Renger, T. *Photosynth. Res.* **2009**, *102*, 471−485.